Amorphization of C60 nanotubes under pressure

J. Y. Hu, S. C. Liang, G. Z. Piao, S. J. Zhang, Q. H. Zhang et al.

Related Articles

Tricritical behavior of the RI–RV rotator phase transition in a mixture of alkanes with nanoparticles
J. Chem. Phys. 135, 134505 (2011)

Pressure-induced amorphization in mayenite (12CaO·7Al2O3)
J. Chem. Phys. 135, 094506 (2011)

Influence of Al2O3 crystallization on band offsets at interfaces with Si and TiNx
Appl. Phys. Lett. 99, 072103 (2011)

Temperature induced transition from hexagonal to circular pits in graphite oxidation by O2
Appl. Phys. Lett. 99, 044102 (2011)

Phase transformation of Ho2O3 at high pressure
J. Appl. Phys. 110, 013526 (2011)

Additional information on J. Appl. Phys.

Amorphization of C_{60} nanotubes under pressure

J. Y. Hu,[1,2] S. C. Liang,[3] G. Z. Piao,[3] S. J. Zhang,[1] Q. H. Zhang,[1] Y. Yang,[1] Q. Zhao,[2] K. Zhu,[1] Y. L. Liu,[1] L. Y. Tang,[4] Y. C. Li,[4] J. Liu,[4] C. Q. Jin,[1] and R. C. Yu[1,a)]

[1]*Beijing National Laboratory for Condensed Matter Physics, Institute of Physics, Chinese Academy of Sciences, P. O. Box 603, Beijing 100190, People's Republic of China*
[2]*Department of Physics, School of Science, Beijing Institute of Technology, Beijing 100081, People's Republic of China*
[3]*Key Laboratory of Rubber-plastics, Ministry of Education, Qingdao University of Science and Technology, Qingdao 266042, People's Republic of China*
[4]*Institute of High Energy Physics, Chinese Academy of Sciences, Beijing 100039, People's Republic of China*

C_{60} nanotubes with diameters of smaller than 500 nm are fabricated by a modified liquid–liquid interfacial precipitation method. *In situ* angle dispersive synchrotron x ray diffraction and Raman scattering under pressures have been employed to study the structure evolution of the C_{60} nanotubes. The experimental results indicate that there is a pressure induced irreversible amorphization at 40.1 GPa. An isostructural phase transition occurs in the pressure range of 9.29–12.2 GPa, which is probably relative to the changes in the bonding type of C_{60} nanotubes. © *2011 American Institute of Physics*. [doi:10.1063/1.3601740]

I. INTRODUCTION

Since the discovery by Kroto *et al.*,[1] fullerene materials (C_{60}, C_{70}, etc.) with a distinctive symmetrical carbon cage structure have been extensively studied due to its unique physical and chemical characteristics and its potential applications in various fields. Recently, one-dimensional fullerene nanostructures, such as wires, rods, and tubes, have attracted much attention, owing to their potential applications in nanoscale devices.[2] To synthesize highly crystallized C_{60} one-dimensional nano-material, a modified liquid–liquid interfacial precipitation (LLIP) method has been used. Later, pure fullerene nanowhiskers with hollow structures, which could be called as fullerene nanotubes, have been fabricated by this method.[3–6] These nanotubes, with diameters smaller than 1000 nm and several millimeters in length, could be re-dissolved in proper solvents, so they may be useful not only as adsorbents and catalysts but also as templates for the various forms of materials, such as fibers and membranes.[7] Although some assumptions have been proposed to explain the tubular morphology of these fullerene nanotubes, until now, the formation mechanism of the tubular structures was not fully understood.[3–6,8]

As well known, the physical properties of a material are determined by its structure. High pressure, as a new dimension, can tune the crystal structures and electronic structures of materials and further their physical properties. Molecular crystals are very sensitive to high pressure, since the intermolecular bonds in them are easily compressed, and the molecules themselves may also be modified under pressure.[9,10] Recently, the interest in understanding the high pressure phases of graphite has been further extended to some carbon allotropes, for example, C_{60} fullerene, a typical molecular crystal. The single C_{60} molecule has been calculated to have an extremely large bulk modulus B_0 of 700–900 GPa,[11,12]

which greatly exceeds that of diamond ($B_0 = 442$ GPa). However, under atmospheric pressure and temperature, the pristine C_{60} crystal, which is characterized by weak van der Waals interaction between the C_{60} molecules, results in a soft solid with the bulk modulus B_0 ranged from 12.8 to 22.2 GPa, and the pressure dependence of bulk modulus (dB/dP) is 5.7 ± 0.6.[13–16] But nano-crystallites exhibit significantly different properties from the bulk material under pressure, such as phase transitions and the bulk modulus.[17–20] It was reported that a pressure induced transformation from sp^2 to sp^3 hybridization happens in C_{60} around 13 GPa and, in multi-walled carbon nanotubes, around 16 GPa.[21] The synthesis and the bulk modulus of C_{60} nanosheets were also discussed by Wang *et al.*[22] and it was found that the C_{60} nanosheets have a larger bulk modulus than the bulk crystals.

Recently, due to the unique molecular structure of C_{60} and the versatility of its phonon spectrum, Raman scattering has been widely used in investigating the physical properties and phase transitions of fullerene-based materials,[23–25] especially coupled with the application of external pressure.[26–28] In this paper, we report the structural stability of the C_{60} fullerene nanotubes under pressure, which were fabricated by LLIP, by using an *in situ* high pressure angle dispersive synchrotron x ray diffraction (AD-XRD) experiment and Raman scattering measurements.

II. EXPERIMENTS

The C_{60} nanotubes are fabricated by LLIP. As reported elsewhere,[3–5,7] the pristine C_{60} powder (MTR Ltd. 99.5%) was dissolved in pyridine, and then the pyridine solution of C_{60} was added to isopropyl alcohol in a proper mixture ratio. One min ultrasonic dispersion was taken to obtain suitable diffusion at the interface. In order to promote the growth of the C_{60} nanotubes, the solutions were exposed to visible light, such as blue light with a center wavelength of 468 nm.[4,5] The hollow structure of the C_{60} nanotubes was characterized using

a)Author to whom correspondence should be addressed. Electronic mail: rcyu@aphy.iphy.ac.cn.

a transmission electron microscope (TEM, JEM-2000EX). In the TEM experiments, the specimens were placed on a copper micro grid with carbon film.

In situ high pressure AD-XRD measurements up to about 40.1 GPa were performed at Beijing Synchrotron Radiation Facility (BSRF) at ambient temperature. The x ray wavelength was 0.06199 nm, and the beam size was 25 μm in diameter. The diffracted x ray was detected with an imaging plate. High pressure was generated using a symmetric-type DAC with 300 μm culets. The sample was loaded into the sample chamber in the T301 stainless steel gasket, and the pressure was measured by using the ruby fluorescence technique.[29]

In situ high pressure Raman scattering measurements up to about 35.7 GPa, also using DAC technique, were carried out on a LABRAM-HR confocal laser Micro-Raman spectrometer (HR800). Raman spectra were recorded in back-scattering geometry in the frequency region from 100 to 4000 cm^{-1}. The 532 nm line of the Verdi-2 solid-state laser was used as a Raman excitation source. A 25 × microscope objective lens was applied in order to focus the laser beam and collect the scattered light. The instrument resolution was 1 cm^{-1}. All the measurements were carried out at room temperature.

III. RESULTS AND DISCUSSION

A typical hollow image of the C_{60} nanotubes is shown in Fig. 1. The tubular structure is clearly revealed, diameters of the sample are smaller than 500 nm, and the lengths exceed several micrometers.

The C_{60} nanotubes have different morphologies in different circumstances. In the process of synthesis of the C_{60}
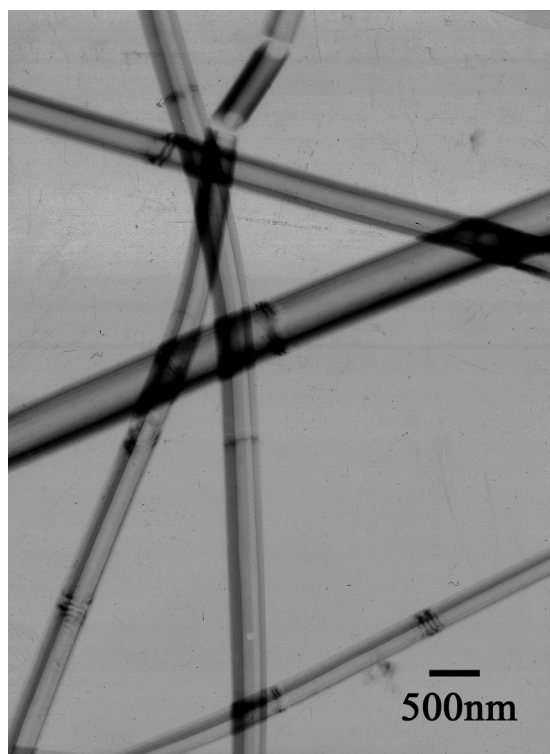
nanotubes by the LLIP method,[7,8,30] the C_{60} nanotube shows a hexagonal structure with a space group of P6$_3$/mmc and cell parameters of $a = 1.541$ nm and $c = 1.00$ nm[8] in solution, while it has a fcc structure with a space group of Fm3m and cell constant of $a = 1.424$ after being completely dried at room temperature.[8]

The AD-XRD patterns of the C_{60} nanotubes at different pressures are shown in Fig. 2(a). The peaks can be indexed to the fcc structure. The peaks become broad compared to those of the pristine C_{60}, due to a nanosize effect. With increasing pressure, the diffraction peaks become broader and weaker and gradually shift to larger angles, showing the compression of the lattice. When the pressure increases to 9.79 GPa, the 511 peak disappears. And, as the pressure reaches 26.6 GPa, the 111 and 311 peaks also disappear, and the 220 and 420 peaks become much broader and weaker. When the pressure reaches 40.1 GPa, all the peaks vanish; instead, only a broad band occurs, indicating that the fcc structure of the C_{60} nanotubes transforms into an amorphous structure. When pressure is released to ambient pressure, the original fcc peaks are not recovered and the broad band is quenched, indicating that the phase transition is irreversible.

Figure 2(b) shows the unit cell volume of the C_{60} nanotubes as a function of pressure, where the solid lines are the fitting results using Birch–Murnaghan equation:[31]

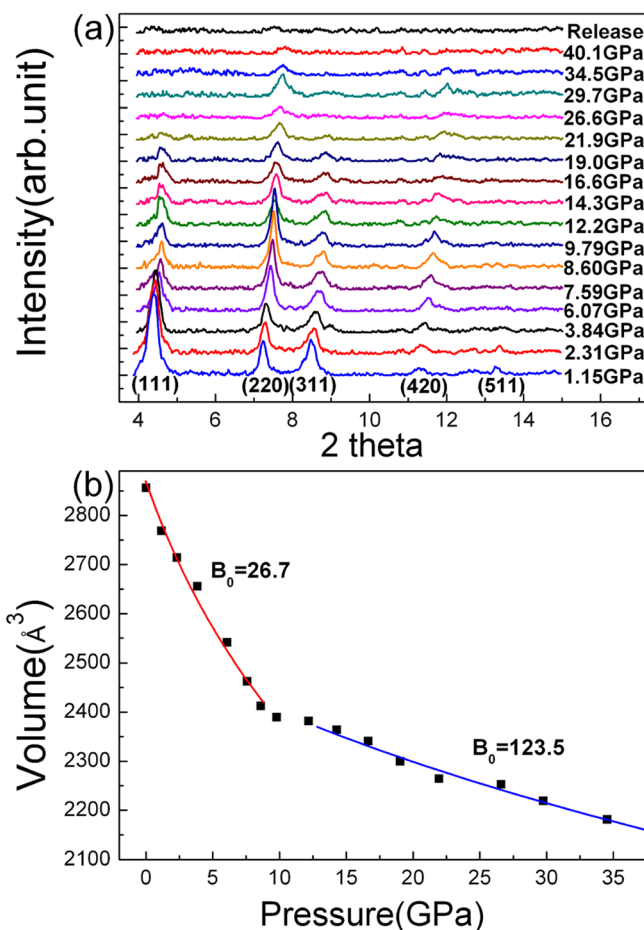FIG. 1. TEM image of the C_{60} nanotubes.

FIG. 2. (Color online) (a) AD-XRD patterns of C_{60} nanotubes at different pressures; (b) pressure dependence of the unit cell volume. The solid lines in (b) are the fitting results according to the Birch-Murnaghan equation of state.

$$P = \frac{3}{2} B_0 \left[\left(\frac{V}{V_0}\right)^{-\frac{7}{3}} - \left(\frac{V}{V_0}\right)^{-\frac{5}{3}} \right]$$

$$* \left\{ 1 - \frac{3}{4}(4 - B_0') \left[\left(\frac{V}{V_0}\right)^{-\frac{2}{3}} - 1 \right] \right\}.$$

From Fig. 2(b), it can be seen that the bulk moduli show different values below 9.79 GPa and above 12.2 GPa, so we fit the two parts individually. With the pressure derivative B_0' fixed as 4, the bulk moduli $B_0 = 26.7$ GPa below 9.79 GPa and $B_0 = 123.5$ GPa above 12.2 GPa are obtained. There is no structural type transition before the transformation to the amorphous except the discontinuity of the derivative of the unit cell volume with pressure, which indicates an isostructural phase transition occurring at about 9.79 GPa. At about 12.2 GPa, the C_{60} nanotubes completely transform to a high-pressure fcc (HPC) structure from the primary low-pressure fcc (LPC) structure. We suppose that this pressure induced isostructural phase transition in the range of 9.29-12.2 GPa may result from the changes in the bonding type, which is similar to the result that the bonding type in C_{60} completely transforms to sp^3 type around 13 GPa.[21] The transformation to sp^3 type bonding from sp^2 is also confirmed in our Raman scattering experiments described below.

In order to further confirm the pressure induced amorphous phase transition of C_{60} nanotubes, we performed *in situ* high pressure Raman scattering measurements. In Fig. 3, we display the Raman scattering spectra at different pressures up to 35.7 GPa at room temperature in two frequency regions 200–1200 and 1400–2000 cm^{-1} due to the appearance of strong Raman peak of diamond at 1333 cm^{-1}. As shown in Fig. 3, the Raman spectrum of C_{60} nanotubes at 0.47 GPa contains the same ten Raman active modes (2 Ag and 8 Hg) as pristine C_{60};[32] we obtained almost all of them except the Hg(6) mode at 1254 cm^{-1}, which is completely covered up by the strong peak of diamond. The additional Raman modes at 526 cm^{-1} and 955 cm^{-1} are relative to the polymerization of C_{60} molecules.[33] With increasing pressure, the Hg and Ag peaks become broader and weaker, and the Hg(5) mode at

FIG. 3. (Color online) Raman spectra of the C_{60} nanotubes at different pressures.

1106 cm^{-1} disappears at 2.86 GPa and the Hg(2) mode at 430 cm^{-1} vanishes at 8.15 GPa. When the pressure reaches 13.0 GPa, where the pressure is just above the isostructural phase transition pressure range of 9.79$-$12.2 GPa obtained in AD-XRD, the Ag(1) mode at 430 cm^{-1} and Hg(7) mode at 1427 cm^{-1} disappear. At 16.7 GPa, the Hg(1) mode at 270 cm^{-1} completely disappears, and the relative intensities of the two peaks Ag(2) at 1463 cm^{-1} and Hg(8) at 1570 cm^{-1} reverses. As the pressure reaches 28.9 GPa, all the Hg and Ag peaks are invisible; instead, the Raman spectrum becomes a broad band, indicating the amorphization of the C_{60} nanotubes. With increasing pressure up to 35.7 GPa, the spectra stays similar. When the pressure releases to ambient pressure, there are three broad bands with widths exceeding 70 cm^{-1} that appear at 710 cm^{-1}, 1443 cm^{-1} and 1560 cm^{-1}, indicating that some parts of C_{60} nanotubes revert to have the characters of the fcc structure but keep very short range of order. This is the reason why the AD-XRD pattern obtained after releasing pressure still shows an amorphous structure. Consistent with Yoo *et al.*,[34] in the pressure released curve, a band at 1560 cm^{-1}, the down shift of which is from the frequency of sp^2 C$=$C stretchings, typically 1580$-$1600 cm^{-1}, is due to formation of the interball sp^3 C–C bonding. This result is consistent with the observation of the isostructural phase transition in our AD-XRD experiments.

IV. CONCLUSIONS

In summary, we fabricated the pure C_{60} nanotubes using the LLIP method, and carried out *in situ* AD-XRD and Raman scattering measurements under pressures to study the structure evolution of the C_{60} nanotubes. Pressure induced amorphization was observed in both experiments. When the pressure releases to ambient pressure, the AD-XRD experiment shows the amorphization is irreversible, and the Raman spectra indicates that some parts of the C_{60} nanotubes revert to have the characteristics of the fcc structure, but keep very short range of order, which induces no Bragg peaks in the AD-XRD pattern. The Raman experiment results show the evidence of the occurrence of an isostructural phase transition observed in the AD-XRD experiment in the pressure range of 9.29–12.2 GPa, which is probably caused by the changes in the bonding type of C_{60} nanotubes.

ACKNOWLEDGMENTS

This work was supported by the National Natural Science Foundation of China (Grant Nos. 50921091 and 50773033), the State Key Development Program for Basic Research of China (Grant No. 2005CB623602), and the specific funding of Discipline and Graduate Education Project of Beijing Municipal Commission of Education.
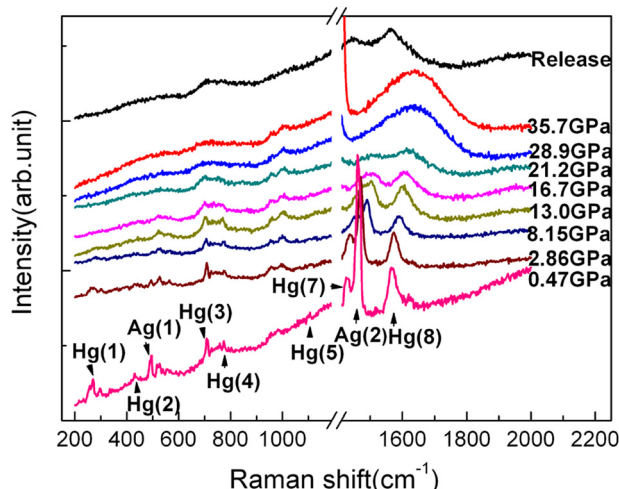
[1]H. W. Kroto, J. R. Heath, S. C. Obrien, R. F. Curl, and R. E. Smalley, Nature **318**, 162 (1985).
[2]Y. N. Xia, P. D. Yang, Y. G. Sun, Y. Y. Wu, B. Mayers, B. Gates, Y. D. Yin, F. Kim, and Y. Q. Yan, Adv. Mater. **15**, 353 (2003).
[3]K. Miyazawa, J. Minato, T. Yoshii, M. Fujino, and T. Suga, J. Mater. Res. **20**, 688 (2005).
[4]G. Z. Piao, G. B. Li, P. Liu, Z. Han, J. Zhao, S. X. Li, and G. Y. Liu, Mater. Lett. **64**, 483 (2010).

Downloaded 17 Nov 2011 to 159.226.35.216. Redistribution subject to AIP license or copyright; see http://jap.aip.org/about/rights_and_permissions

[5] G. Z. Piao, Y. T. Qu, S. C. Liang, K. Zou, S. X. Li, L. M. Liu, and J. A. Zhao, Mater. Lett. **65**, 562 (2011).

[6] G. Z. Piao, G. B. Li, Z. Han, J. Zhao, S. X. Li, and G. Y. Liu, Mater. Sci. Eng., B **163**, 161 (2009).

[7] J. Minato, K. Miyazawa, and T. Suga, Sci. Technol. Adv. Mater. **6**, 272 (2005).

[8] J. Minato and K. Miyamwa, Diamond Relat. Mater. **15**, 1151 (2006).

[9] R. Custelcean and Z. A. Dreger, J. Phys. Chem. B **107**, 9231 (2003).

[10] E. V. Boldyreva, J. Mol. Struct. **647**, 159 (2003).

[11] S. J. Woo, S. H. Lee, E. Kim, K. H. Lee, Y. H. Lee, S. Y. Hwang, and I. C. Jeon, Phys. Lett. A **162**, 501 (1992).

[12] R. S. Ruoff and A. L. Ruoff, Nature **350**, 663 (1991).

[13] O. Blaschko, W. Rom, and I. N. Goncharenko, J. Phys. Condens. Matter **8**, 4235 (1996).

[14] S. J. Duclos, K. Brister, R. C. Haddon, A. R. Kortan, and F. A. Thiel, Nature **351**, 380 (1991).

[15] J. E. Fischer, P. A. Heiney, A. R. Mcghie, W. J. Romanow, A. M. Denenstein, J. P. Mccauley, and A. B. Smith, Science **252**, 1288 (1991).

[16] A. Lundin, B. Sundqvist, P. Skoglund, A. Fransson, and S. Pettersson, Solid State Commun. **84**, 879 (1992).

[17] S. B. Qadri, J. Yang, B. R. Ratna, E. F. Skelton, and J. Z. Hu, Appl. Phys. Lett. **69**, 2205 (1996).

[18] S. H. Tolbert and A. P. Alivisatos, J. Chem. Phys. **102**, 4642 (1995).

[19] H. Abruna, L. Larrimore, S. Nad, X. J. Zhou, and P. L. McEuen, Nano Lett. **6**, 1329 (2006).

[20] H. Trotter, R. Philips, B. Ni, Y. H. Hu, S. B. Sinnott, P. T. Mikulski, and J. A. Harrison, J. Nanosci. Nanotechnol. **5**, 536 (2005).

[21] R. S. Kumar, M. G. Pravica, A. L. Cornelius, M. F. Nicol, M. Y. Hu, and P. C. Chow, Diamond Relat. Mater. **16**, 1250 (2007).

[22] L. Wang, B. B. Liu, D. D. Liu, M. G. Yao, S. D. Yu, Y. Y. Hou, B. Zou, T. Cui, G. T. Zou, B. Sundqvist, Z. J. Luo, H. Li, Y. C. Li, J. Liu, S. J. Chen, G. R. Wang, and Y. C. Liu, Appl. Phys. Lett. **91**, 103112 (2007).

[23] P. H. M. Vanloosdrecht, P. J. M. Vanbentum, and G. Meijer, Phys. Rev. Lett. **68**, 1176 (1992).

[24] A. M. Rao, P. Zhou, K. A. Wang, G. T. Hager, J. M. Holden, Y. Wang, W. T. Lee, X. X. Bi, P. C. Eklund, D. S. Cornett, M. A. Duncan, and I. J. Amster, Science **259**, 955 (1993).

[25] D. W. Snoke, Y. S. Raptis, and K. Syassen, Phys. Rev. B **45**, 14419 (1992).

[26] K. P. Meletov, D. Christofilos, S. Ves, and G. A. Kourouklis, Phys. Rev. B **52**, 10090 (1995).

[27] G. A. Kourouklis, S. Ves and K. P. Meletov, Physica B **265**, 214 (1999).

[28] R. Poloni, D. Machon, M. V. Fernandez-Serra, S. Le Floch, S. Pascarelli, G. Montagnac, H. Cardon, and A. San-Miguel, Phys. Rev. B **77**, 125413 (2008).

[29] H. K. Mao, J. Xu, and P. M. Bell, J. Geophys. Res. **91**, 4673 (1986).

[30] J. Minato and K. Miyazawa, Carbon **43**, 2837 (2005).

[31] L. Gerward, J. Phys. Chem. Solids **46**, 925 (1985).

[32] R. A. Jishi, R. M. Mirie, and M. S. Dresselhaus, Phys. Rev. B **45**, 13685 (1992).

[33] R. Moret, P. Launois, T. Wagberg, and B. Sundqvist, Eur. Phys. J. B **15**, 253 (2000).

[34] C. S. Yoo and W. J. Nellis, Chem. Phys. Lett. **198**, 379 (1992).